International Journal of Climatology

International Journal of Climatology | RMetS

RESEARCH ARTICLE OPEN ACCESS

Multi-Country-Multi-City Characterisation of Heat Stress and Exposure in Africa

Tobi Eniolu Morakinyo[1] | Oluwafemi E. Adeyeri[2,3] | Mojolaoluwa Toluwalase Daramola[4] | Bobde Vishal[5] | Kazeem Abiodun Ishola[4,6] | Oluwafemi Benjamin Obe[7] | Emmanuel Olaoluwa Eresanya[4,8] | Akintomide Afolayan Akinsanola[5] | Charles Onyutha[9] | Brian Odhiambo Ayugi[10] | Patricia Nying'uro[11,12]

[1]Department of Geography, Texas A&M University, College Station, Texas, USA | [2]Fenner School of Environment and Society, The Australian National University, Canberra, Australia | [3]ARC Centre of Excellence for the Weather of the 21st Century, The Australian National University, Canberra, Australia | [4]Irish Climate Analysis Research Units (ICARUS), department of Geography, Maynooth University, Co. Kildare, Ireland | [5]Department of Earth and Environmental Sciences, University of Illinois Chicago, Chicago, Illinois, USA | [6]National Centre for Geocomputation, Maynooth University, Maynooth, Ireland | [7]Department of Civil, Structural and Environmental Engineering, Trinity College Dublin, Dublin, Ireland | [8]Organization of African Academic Doctors (OAAD), Nairobi, Kenya | [9]Department of Civil and Environmental Engineering, Kyambogo University, Kyambogo, Uganda | [10]East Africa Hub, Wyss Academy for Nature at the University of Bern, Nanyuki, Kenya | [11]Kenya Meteorological Department, Nairobi, Kenya | [12]Oeschger Centre for Climate Change Research, Bern, Switzerland

Correspondence: Tobi Eniolu Morakinyo (tobi.morakinyo@tamu.edu)

Received: 30 August 2025 | **Revised:** 4 April 2026 | **Accepted:** 8 April 2026

Keywords: Africa | bioclimatology | ERA5-UTCI | heat | heat stress | thermal comfort

ABSTRACT

This study presents the first continent-wide assessment of long-term (1974–2023) summer heat stress in Africa using the Universal Thermal Climate Index (UTCI) derived from ERA5-HEAT reanalysis datasets. Employing a grid-specific definition of summer, we analysed UTCI trends across spatial (continental to city scale) and temporal (decadal to hourly) dimensions. While annual UTCI anomalies range 0.2°C–1.6°C, substantial intensification emerges at finer scales. The frequency, duration and spatial extent of 'very strong' (38°C–46°C) and 'extreme' (≥46°C) heat stress have increased markedly, particularly, in the Sahel. Heat-stressed hours (UTCI > 32°C) rose by 2%–25% across most countries, with extreme events doubling in 3–5 and 6–8 days episodes. City-level analyses reveal escalating risks in large urban centres like Cairo, Lagos and Kano. As climate projections indicate further intensification, the findings underscore the urgent need for targeted heat-health adaptation and early warning systems to protect vulnerable populations across the continent.

1 | Introduction

Climate change is a key driver of increasing human heat stress, defined as the physiological burden that occurs when the body can no longer maintain thermal equilibrium under extreme environmental conditions. Heat stress is shaped by the combined effects of air temperature, humidity, wind speed and solar radiation (Morakinyo et al. 2019; Parkes et al. 2022). As global temperatures rise, heatwaves are projected to become more frequent, longer and more intense, increasing the risk of heat stress, other heat-related illnesses and mortality (Ebi et al. 2021; Olaoluwa et al. 2022; Adeyeri, Zhou, et al. 2025).

To quantify this multifactorial heat stress, over 35 thermal indices, such as the Heat Index, Temperature-Humidity Index, Apparent Temperature, Wet-Bulb Globe Temperature, Universal Thermal Climate Index (UTCI) and so forth, have been developed since 1905 (Fiala et al. 2012; Manyuchi et al. 2022). Among these, UTCI has emerged as one of the most physiologically representative and comprehensive tool for assessing

human heat stress and thermal (dis)comfort. The index incorporates a dynamic thermoregulatory model of the human body and accounts for clothing insulation that varies with temperature, enabling more realistic assessments of thermal comfort and population exposure (Bröde et al. 2012; Fiala et al. 2012). UTCI-based historic-to-current assessments indicate growing exposure to 'very strong' heat stress across African regions such as Nigeria (Morakinyo et al. 2024), Southern Africa (Roffe et al. 2023), Northern Africa (Hamed et al. 2024) and the entire African continent (Adeyeri, Ajadi, et al. 2025). The variation over the continent can be attributed to several factors, including geographic and socio-economic ones. In Northern Africa, particularly in rapidly growing cities in Egypt and Algeria, the population faces heightened risks due to climate change and urbanisation, which are compounded by inadequate adaptation strategies (Parkes et al. 2022). Southern Africa experiences both seasonal and long-term shifts in heat stress, with cold stress in the winter and pronounced heat stress in the summer (Roffe et al. 2023). Equatorial regions and the Sahel are projected to see unprecedented increases in heat stress under global warming scenarios predicting temperature rises of 2°C or more (Sylla et al. 2018; Vecellio et al. 2023). Generally, heat stress in urban areas is often exacerbated by the urban heat island (UHI) effect. As African cities experience rapid population growth, urban expansion and rising informal settlements, UHI intensity and spatial extent can increase, aggravating heat-related morbidity and mortality and, in some contexts, contributing to social strain (Gyimah 2023; Morakinyo et al. 2026). Beyond health impacts, rising heat intensity and shifting spatial coverage also threaten agriculture through compounding heat and drought extremes, which are projected to worsen under 2°C of global warming (Muheki et al. 2024). Heat stress further undermines labour productivity and urban resilience, with, particularly, severe implications for Africa, where high exposure and low adaptive capacity amplify climate vulnerability (Adigun et al. 2024; Akinsanola et al. 2025).

Distinct atmospheric factors also shape heat stress patterns across Africa. High-pressure systems contribute to prolonged dry periods, elevating temperatures and reducing humidity, thereby intensifying dry heat stress in arid regions, while heightened humidity intensifies moist heat stress (Baldwin et al. 2023; Guigma et al. 2020). The Sahel and the Horn of Africa face extreme heat exposure due to arid conditions, while parts of Southern Africa exhibit varying levels of heat stress (Ncongwane, Botai, Sivakumar, Botai, et al. 2021) due to the combined effect of the high prevalence of high-pressure systems, intense solar radiation and high sensible heat from dried sandy surfaces, while artificial surfaces in urban areas exacerbate local warming (Adeyeri et al. 2024). Heat stress in Southern Africa is strongly influenced by climate variability phenomena, particularly, the effects of El Niño and La Niña (Roffe et al. 2023). Changes in wind patterns driven by sea surface temperature anomalies further exacerbate inland heating, increasing heat extremes in previously temperate regions (Adigun et al. 2024; Mitchell et al. 2021). These climatic dynamics interact with local factors such as soil moisture levels and vegetative cover, making heat stress impacts highly variable and complex. Land-use changes, including deforestation and agricultural expansion and urbanisation also exacerbate this risk as expanding cities create UHIs, significantly raising local temperatures (Li et al. 2022; Parkes et al. 2022) and also contribute to frequent extreme heat events (Adeyeri et al. 2023). Specifically, agricultural practices modulate regional temperatures primarily through their influence on soil moisture and evapotranspiration. Land-use changes such as agricultural expansion and deforestation can intensify regional warming by reducing evapotranspiration and shifting the surface energy balance towards greater sensible heat flux. Soil drying limits plant transpiration, suppresses evaporative cooling and promotes atmospheric heating, thereby exacerbating heatwave intensity and persistence. In contrast, adequate soil moisture provides important cooling feedback by enhancing latent heat flux and moderating extreme temperatures. Consequently, land management strategies that promote soil moisture retention—such as agroforestry and sustainable groundwater management—can play a critical role in reducing heatwave frequency and severity (Adeyeri, Zhou, et al. 2025).

Under high-emission scenarios such as RCP8.5 and SSP 585, heat stress exposure across Africa is expected to rise dramatically, necessitating urgent adaptation measures (Fotso-Nguemo et al. 2022; Parkes et al. 2019; Adeyeri, Ajadi, et al. 2025). Across Africa, projected trends reveal increasing occurrences of moderate to 'very strong' heat stress, driven by both rising ambient and apparent temperatures. These trends are particularly severe in densely populated urban regions, where anthropogenic surfaces and inadequate infrastructure exacerbate warming (Dajuma et al. 2024; Fotso-Nguemo et al. 2022). West and northern East Africa have experienced some of the most significant increases in the frequency and duration of extreme heat events, with projections suggesting that many West African cities could reach 'extreme caution' or 'danger' heat stress thresholds by mid-century (Dajuma et al. 2024; Fotso-Nguemo et al. 2022; Roffe et al. 2023).

Overall, previous studies have primarily focused on understanding the spatio-temporal trends and patterns of heat stress in specific countries or regions, including Nigeria (Benjamin Obe et al. 2023; Morakinyo et al. 2024), Southern Africa (Roffe et al. 2023), South Africa (Ncongwane, Botai, Sivakumar, Botai, Adeola 2021), North Africa and the Arabian Peninsula (Hamed et al. 2024), the Great Lakes Region (Asefi-Najafabady et al. 2018) and the Sahelian region (Guigma et al. 2020). Other studies have examined heatwave or hot extremes trends, patterns, atmospheric drivers and societal impacts (Adigun et al. 2024; Guigma et al. 2020; Igun et al. 2022; Adeyeri, Ajadi, et al. 2025; Bobde, Ayegbusi, et al. 2025; Bobde, Akinsanola, et al. 2025). However, there has been limited or no comprehensive study on the characterisation of historical heat stress and its spatio-temporal trends across the entire African continent. This gap is critical because, while heatwaves and extreme temperatures serve as proxies for heat stress, they are temperature-based indicators that do not fully capture the physiological strain imposed on humans (Adeyeri et al. 2023). Furthermore, most prior studies on heat (waves) have traditionally defined the summer period using fixed 3-month windows based on boreal (Northern Hemisphere) and austral (Southern Hemisphere) summers. However, this approach overlooks local variations in the hottest months, particularly near the equator, where peak solar radiation shifts due to north–south migration. As a result, discrepancies in summer definitions across sub-regions can introduce biases, failing to accurately capture the true summer period in some locations.

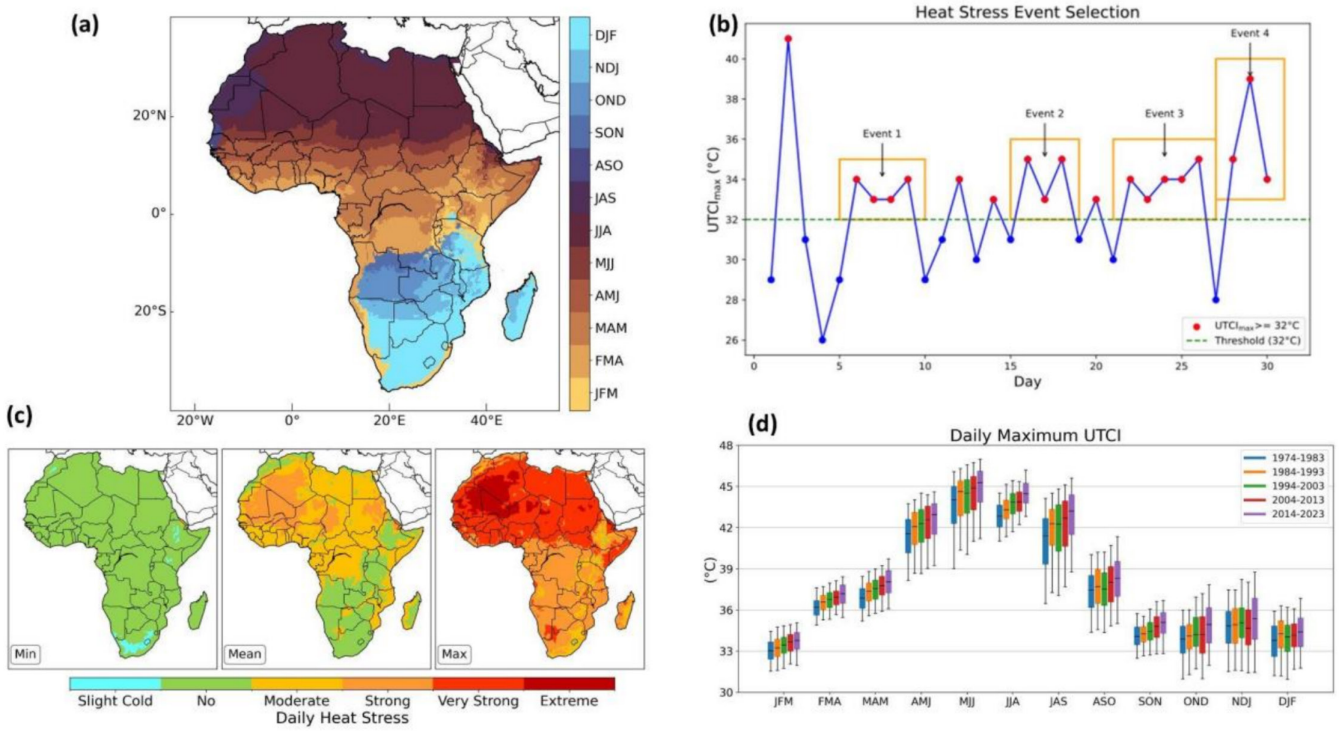

FIGURE 1 | (a) Grid-specific summer season identification based on long-term (1974–2023) climatology of monthly UTCI, highlighting the hottest 3 months per grid cell using distinct colour shades; (b) heat stress event selection method based on non-overlapping consecutive days where $UTCI_{max} \geq 32°C$; (c) long-term average (1974–2023) spatial patterns and magnitudes of minimum, mean and maximum heat stress during Africa's summer periods; (d) distribution of maximum UTCI values across different summer months, showing regional variation in peak heat stress. [Colour figure can be viewed at wileyonlinelibrary.com]

To address this limitation, we adopt a recently developed 'grid-specific' summer definition (Bobde, Ayegbusi, et al. 2025; Bobde, Akinsanola, et al. 2025)—that is, the grid-specific climatological hottest 3 months based on the long-term (1974–2023) monthly UTCI climatology—for data analysis and visualisation. Therefore, using these grid-specific summer months across our region of interest, Africa (Figure 1a), we extracted hourly UTCI data for the period 1974–2023, enabling a continent-wide analysis of heat stress during summer periods. This method ensures that heat stress is assessed using the most relevant seasonal period for each grid. This study is the first to comprehensively investigate the historical climatology of heat stress across Africa. The specific objectives include (1) investigating the historical and current spatio-temporal patterns of 'grid-specific' summer UTCI classes across Africa; (2) conducting a trend analysis of UTCI anomalies based on grouped grid-specific summer and consecutive days and hours of heat stress per year and (3) performing continental- and city-level analyses of heat stress, exposure and vulnerability, with a focus on cities with populations ≥ 1 million.

2 | Methods

2.1 | ERA5-HEAT Data Description

The ERA5-HEAT reanalysis dataset, developed by the European Centre for Medium-Range Weather Forecasts (ECMWF), represents a major advance in the availability, consistency and accuracy of spatially gridded historical data for assessing human thermal comfort and heat stress. It provides hourly records of the UTCI and mean radiant temperature (MRT) on a $0.25° \times 0.25°$ grid and spans from 1940 to the present, enabling assessment of long-term trends in human thermal conditions at the global scale (Di Napoli et al. 2021). UTCI is a bioclimatic index that quantifies human physiological responses to meteorological conditions and is computed using MRT, 2 m air temperature and dew-point temperature (to compute relative humidity) and 10 m zonal and meridional winds (to calculate wind speed) derived from the ERA5 reanalysis product (Hersbach et al. 2020).

The MRT is calculated using both solar and thermal radiation fluxes. Thermal radiation consists of the downwelling radiation from the atmosphere and upwelling radiation from the surface. Solar radiation is split into a direct component from the sun and a diffuse component, which includes isotropic diffuse solar radiation flux and surface-reflected solar radiation flux (Di Napoli et al. 2021, 2023). These fluxes are combined to calculate MRT, which is essential for capturing the impact of radiant energy on the human body. The derived MRT is integrated with other atmospheric data to calculate the UTCI using the Fiala model, which has become an established method for assessing human thermal stress and understanding how individuals experience extreme climate conditions (Błazejczyk et al. 2013; Bröde et al. 2012; Fiala et al. 2012; Bonell et al. 2022, 2023). The ERA5-HEAT dataset has been extensively evaluated and applied across various countries and regions, demonstrating its broad applicability (Bonell et al. 2022, 2023; Krüger and Di Napoli 2022; Morakinyo

et al. 2024; Roffe et al. 2023; Ullah et al. 2024; Urban et al. 2021). For instance, the flagship paper by Di Napoli et al. (2021) conducted extensive comparisons of the UTCI derived from ERA5-HEAT against observations from 177 meteorological stations globally, including 21 across Africa. The results demonstrated strong agreement, with most R^2 values exceeding 0.6 and a high mean value of 0.80 ± 0.13.

Furthermore, a study by Krüger and Di Napoli (2022) in Brazil compared ERA5-HEAT UTCI with in situ observations, yielding an R^2 of 0.64. Notably, when the reanalysis data was compared specifically to measurements from a local World Meteorological Organization (WMO) weather station, the R^2 value improved significantly to 0.85.

In an African context, Morakinyo et al. (2024) found a realistic correlation between ERA5-HEAT UTCI and observations from nine gauge stations across Nigeria. The study concluded that ERA5-HEAT demonstrates reasonable performance in capturing the spatial and temporal characteristics of human thermal and heat stress conditions across a developing country context. Overall, these evaluations indicate that ERA5-HEAT sufficiently captures reference UTCI values, particularly, for coldest and hottest extremes throughout the analysis period.

2.2 | Grid-Based Summer Season-Based Data Selection

Traditionally, the summer period is defined as three fixed months based on the boreal (austral) summer months in the northern (southern) hemisphere. This method fails to account for local variations of the observed hottest months due to north–south migration of the peak solar radiation. This effect is especially true near the equator, where the northern and southern summers do not correspond to the hottest season. Therefore, we propose using grid-specific summer months, which have recently been used to study heatwaves over Africa (Bobde, Ayegbusi, et al. 2025; Bobde, Akinsanola, et al. 2025). In our proposed method of season selection, we first identified the heat stress for three consecutive months based on the long-term (1974–2023) climatology of monthly UTCI at each grid point. After finding the grid-specific summer months over our region of interest—Africa (Figure 1), we used it to extract the hourly UTCI for the period 1974–2023, enabling a continental summer period heat stress analysis.

2.3 | Spatio-Temporal Trend and Pattern Analysis

First, we investigated and compared the spatio-temporal variations of minimum, mean and maximum UTCI (heat stress) severity at a decadal time scale during the summer, using the classification shown in Table 1. We then analysed UTCI trends for each grouped summer period to identify long-term patterns and anomalies following Equations (1–8).

The baseline mean for each city/grid c is defined as follows:

$$\mu_c = \frac{1}{N} \sum_{y=1991}^{2020} H_{c,y} \tag{1}$$

TABLE 1 | Thermal comfort/Heat stress classification based on UTCI value (Błazejczyk et al. 2013).

UTCI range (°C)	Level of thermal stress
< -40	Extreme cold stress
−40 to −27	Very strong cold stress
−27 to −13	Strong cold stress
−13 to 0	Moderate cold stress
0–9	Slight cold stress
9–26	No thermal stress
26–32	Moderate heat stress
32–38	Strong heat stress
38–46	Very strong heat stress
> 46	Extreme heat stress

where $H_{c,y}$ is the number of hours with UTCI ≥ 32°C in year y for grid/city c, μ_c is the baseline climatological mean for grid/city c, N is the number of valid years.

The anomaly, $A_{c,y}$, in year y for grid/city c, relative to 1991–2020 mean, is given as:

$$A_{c,y} = H_{c,y} - \mu_c \tag{2}$$

We calculate the slope using the Theil–Sen estimator (Sen 1968; Theil 1992) for each city/grid c:

$$\beta_c = \text{median}\left(\frac{A_{c,y_j} - A_{c,y_i}}{y_j - y_i}\right), \text{ for all } y_j > y_i \tag{3}$$

Furthermore, we test for monotonic trend significance using the Mann–Kendall test (Kendall 1948; Mann 1945). Let S be the test statistic such that

$$S = \sum_{k=1}^{n-1} \sum_{j=k+1}^{n} Sgn(\theta) \tag{4}$$

where $\theta = \left(A_{c,yj} - A_{c,yi}\right)$ such that $Sgn(\theta) = 1$ if $\theta > 0$, $Sgn(\theta) = 0$ if $\theta = 0$ and $Sgn(\theta) = -1$ if $\theta < 0$and where $A_{c,yj}$and $A_{c,yi}$ are sequential data values for the time series data of length n.

The statistic S is approximately normally distributed with the mean $E(S)$ and the variance $V(S)$ can be computed as (Kendall 1948; Mann 1945).

$$E(S) = 0 \tag{5}$$

$$S = \frac{1}{18} n(n-1)(2n+5) \tag{6}$$

In case there are tied ranks,

$$S = \frac{1}{18}\left(n(n-1)(2n+5) - \sum_{k=1}^{Aq} t_k(k-1)(2k+5)\right) \tag{7}$$

where Aq is the number of tied groups and t_k is the number of observations in the kth group.

The standard normal variate Z is calculated by

$$Z = \begin{cases} \frac{S-1}{\sqrt{V(S)}} \text{if} S > 0 \\ 0 \, if S = 0 \\ \frac{S+1}{\sqrt{V(S)}} \text{if} S < 0 \end{cases} \quad (8)$$

Positive values of Z indicate a rising trend and negative values show a descending trend.

Subsequently, we construct a matrix $A \in \mathbb{R}^{C \times T}$, where C is the number of cities, T is the number of years and each element $A_{c,t}$ represents the anomaly for grid/city c in year t.

Finally, each grid/city has a label indicating

$$\text{Label}_c = \begin{cases} * \beta_{\text{cif } p_c < 0.05} \\ \beta_{\text{cotherwise}} \end{cases} \quad (9)$$

where β_c is the trend slope (hours/year) and * denotes significance at $p < 0.05$.

To calculate the percentage of hours with UTCI ≥ 32°C annually:

$$\text{Percentage} = \left(\frac{above[year]}{total[year]} \right) \times 100 \quad (10)$$

where $total[year]$ is the total number of valid hours in year and $above[year]$ is the number of hours with UTCI ≥ 32°C in year.

The formula for calculating the decadal mean is:

$$\text{Decadal mean}[start\_year, end\_year] = \frac{1}{N} \sum_{t=\text{start\_year}}^{\text{end\_year}} UTCI(t) \quad (11)$$

where N is the number of years in the decadal period and UTCI(t) is the UTCI value for year t.

For the annual percentage calculation:

$$\text{Percentage} = \left(\frac{\sum_{i=1}^{N} above_i}{\sum_{i=1}^{N} total_i} \right) \times 100 \quad (12)$$

where N is the number of years considered, above$_i$ is the number of hours with UTCI ≥ 32°C in year i and total$_i$ is the total valid hours in year i.

2.4 | Statistical Significance Testing

We applied a non-parametric bootstrap procedure to assess whether changes in the percentage of hours with UTCI ≥ 32°C between 1974 and 2023 were statistically significant at the grid-cell level. Instead, for each grid cell, we computed the observed difference between 2023 and 1974 and generated 500 bootstrap replicates by resampling the pair of values with replacement under the null hypothesis of no change. A two-sided p-value was estimated as the proportion of bootstrap replicates with an absolute difference greater than or equal to the observed difference. To control for the elevated risk of false positives associated with conducting thousands of grid-cell-level tests, we implemented the Benjamini–Hochberg false discovery rate (FDR) procedure (Benjamini and Hochberg 1995), which limits the expected proportion of false discoveries. Statistical significance was defined as FDR-adjusted $p < 0.05$. The percentage of significant grid cells was computed for uncorrected and FDR-corrected p-values.

2.5 | Consecutive Heat Stress Days and Hours

Prolonged heat stress, both in terms of days and hours, has significant implications for human health. To understand these changes over time, our subsequent analysis focused on UTCI_{max}, which represents the most severe heat stress conditions. We categorised UTCI_{max} based on levels of heat stress severity (Table 1) and classified events by different durations: 3–5, 6–8, 9–12 and ≥ 13 days.

To identify prolonged heat stress events, we applied a selection algorithm that first detected all days where UTCI_{max} exceeded a threshold X°C (where X corresponds to heat stress categories k, starting from 'strong heat stress' at UTCI ≥ 32°C) (Equation 13). The algorithm then identified and classified consecutive days meeting this criterion (Equation 14) (Figure 1b). This approach allowed us to analyse trends in the severity and duration of heat stress events over time.

$$S_k(i) = \{ 1, \ if \, UTCI_{max,i} \in category_k \ 0, \ \text{otherwise} \quad (13)$$

where $S_k(i)$ corresponds to the heat stress categories $k = 1$: $UTCI_{max} \geq 32$°C, 2: 32°C ≤ $UTCI_{max} < 38$°C, 3: 38°C ≤ $UTCI_{max} < 46$°C and 4: $UTCI_{max} \geq 46$°C.

The Heat Stress Event is defined as follows:

$$\text{Heat Stress Event} = \bigcup_{j=1}^{m} \left(\sum_{i=d_{start}}^{d_{end}} S_k(i) \geq d_{\text{end}} - d_{\text{start}} + 1 \right) \text{ for each } k = 1, 2, 3, 4 \quad (14)$$

where $\sum_{d_{start}}^{d_{end}} S_k$ is the sum of heat stress days for each category within the range $D_j = [d_{start}, d_{end}]$; d_{start} and d_{end} are the start and end of the day range (3–5, 6–8, 9–13, > 13 days); m is consecutive day classification.

To quantify trends in consecutive heat stress days, we applied the non-parametric Mann–Kendall trend test combined with Sen's slope estimator (Sen 1968), which determines the magnitude of change over time. Building on this, we performed a dual-scale assessment—continental and city-level—to evaluate the annual frequency of hours exceeding the 'strong' heat stress threshold (UTCI ≥ 32°C). For city-specific analysis, we focused on Africa's 50 most populous urban centers, using geographic coordinates from Africapolis (Africapolis 2025) to extract UTCI data. Seasonal percentages of hours above the UTCI threshold

were calculated for each city, with decadal averages (1974–2023) visualised to highlight temporal patterns. Spatial trends were mapped to illustrate changes over the 50-year period, overlaid with statistical significance indicators from the Mann–Kendall test. To further contextualise heat stress dynamics, we generated a heatmap depicting the percentage of UTCI ≥ 32°C hours during typical summer months across the study period. Long-term shifts were assessed by aggregating annual heat stress hours (HSH) into summer-period groupings. Finally, we analysed consecutive heat stress episodes by computing the number of sustained hours (UTCI ≥ 32°C) per decade, segmented into five intervals: 1974–1983, 1984–1993, 1994–2003, 2004–2013, 2014–2023.

2.6 | Population-Weighted Exposure

Lastly, we examined population-weighted heat exposure over time and space across different heat stress categories between 2000 and 2020 using the Gridded Population of the World, Version 4 (GPWv4): Population Density dataset (Center For International Earth Science Information Network-CIESIN-Columbia University 2018) and conducted a data sensitivity test by comparing with the Worldpop data (https://www.worldpop.org/).

For each year, we estimated the total population exposed to different levels of heat stress based on the UTCI. Heat stress was categorised into three levels: strong (32°C–38°C), very strong (38°C–46°C) and extreme (> 46°C). To quantify exposure, we calculated the number of days per year that fell within the heat stress category for each spatial grid cell. These values were then weighted by the population in the corresponding grid cell to account for both the frequency of heat stress and the number of people affected.

Population-weighted exposure was computed as follows:

$$E_{c,y} = \sum_{i=1}^{N} D_{i,c,y} \times P_{i,y} \tag{15}$$

where $E_{c,y}$ is the total population exposure (in person-days) for heat stress category c at grid cell i during year y. $D_{i,c,y}$ is the number of days classified under category c at grid cell i during year y, $P_{i,y}$is the population at grid cell i in year y and N is the total number of grid cells considered.

Due to the large variability in population exposure values $E_{c,y}$, we applied a logarithmic normalisation to improve the interpretability of visual outputs.

$$E'_{c,y} = \log 10\left(1 + E_{c,y}\right) \tag{16}$$

This transformation reduces the influence of extremely high values while preserving the relative differences across space and time. For each heat stress category, the change in log-transformed exposure between 2000 and 2020 was subsequently computed and visualised to highlight spatial patterns and temporal trends in population exposure.

3 | Results

3.1 | Spatio-Temporal Pattern of Heat Stress During Grid-Specific Hottest Months

The long-term (1974–2023) average heat stress shown in Figure 1c indicates that the daily minimum UTCI (occurring from nighttime till before sunrise) across Africa during summer is largely categorised as 'No Thermal Stress'. This is because shortwave radiation is low and it is a major driver of MRT, which strongly influences UTCI. The mean UTCI indicates 'moderate' to 'strong' heat stress in locations above the equator and 'No' to 'moderate' stress below the equator. The maximum UTCI, occurring in the afternoon at peak solar intensity, reveals 'very strong' to 'extreme' heat stress in areas above the equator, while areas below generally experience 'strong' conditions—except for the Great Lakes region (which is 'moderate') and the vast Kalahari Desert (which is 'very strong'). Figures S1–S3 show the decadal variations of the minimum, mean and maximum UTCI, respectively. Visually, the spatial patterns have remained relatively unchanged over time; however, more in-depth analysis of the spatio-temporal changes in duration, intensity and occurrence reveals significant shifts. There is a clear distinction between the magnitude of UTCI in the Northern and Southern Hemisphere regions, as expected. Summer heat stress—even at its peak—feels different between the hemispheres, largely due to dominant large-scale systems such as differences in solar intensity (resulting from varying solar angles), high-pressure systems, land cover and land use and atmospheric circulation (Igun et al. 2022; Meque et al. 2022; Roffe et al. 2023). Consequently, summer heat stress conditions in Africa vary by location and prevailing climate, which also dictate the timing of the hottest months. The boxplot in Figure 1d reveals that areas (countries and/or cities) experiencing peak summers in MJJ, JJA and JAS (essentially MJJAS in the Northern Hemisphere) encounter the strongest heat stress. Additionally, UTCI levels have been increasing by decade and the extent and intensity of these changes will be discussed in subsequent sections, where the focus will be on the maximum UTCI due to its severe impact on human health and well-being in Africa (Kunda et al. 2024).

3.2 | Trends in Decadal Anomalies of Daily Maximum UTCI Varies by Summer Period

We analysed spatio-temporal characteristics of decadal anomalies of daily maximum UTCI during 1974–2023, with respect to 30-year (1991–2020) climatology. The patterns for individual decades, based on the derived grid-specific summer season, are presented in Figure 2, S4 and S5. The earlier decades (1974–1983 and 1984–1993) are broadly less heat stressed than the normal summer thermal conditions (negative UTCI anomaly) in summer across the continent but predominantly in Northern Africa, including Algeria, Morocco, Egypt, Sudan and South Sudan. Conversely, a warmer than usual summer heat stress (positive UTCI anomaly) was more widespread in Southern Africa during 1984–1993 compared to other parts of Africa. This is likely determined by positive UTCI values observed in the region for a few years during this decade (see Figure S4 for yearly anomaly

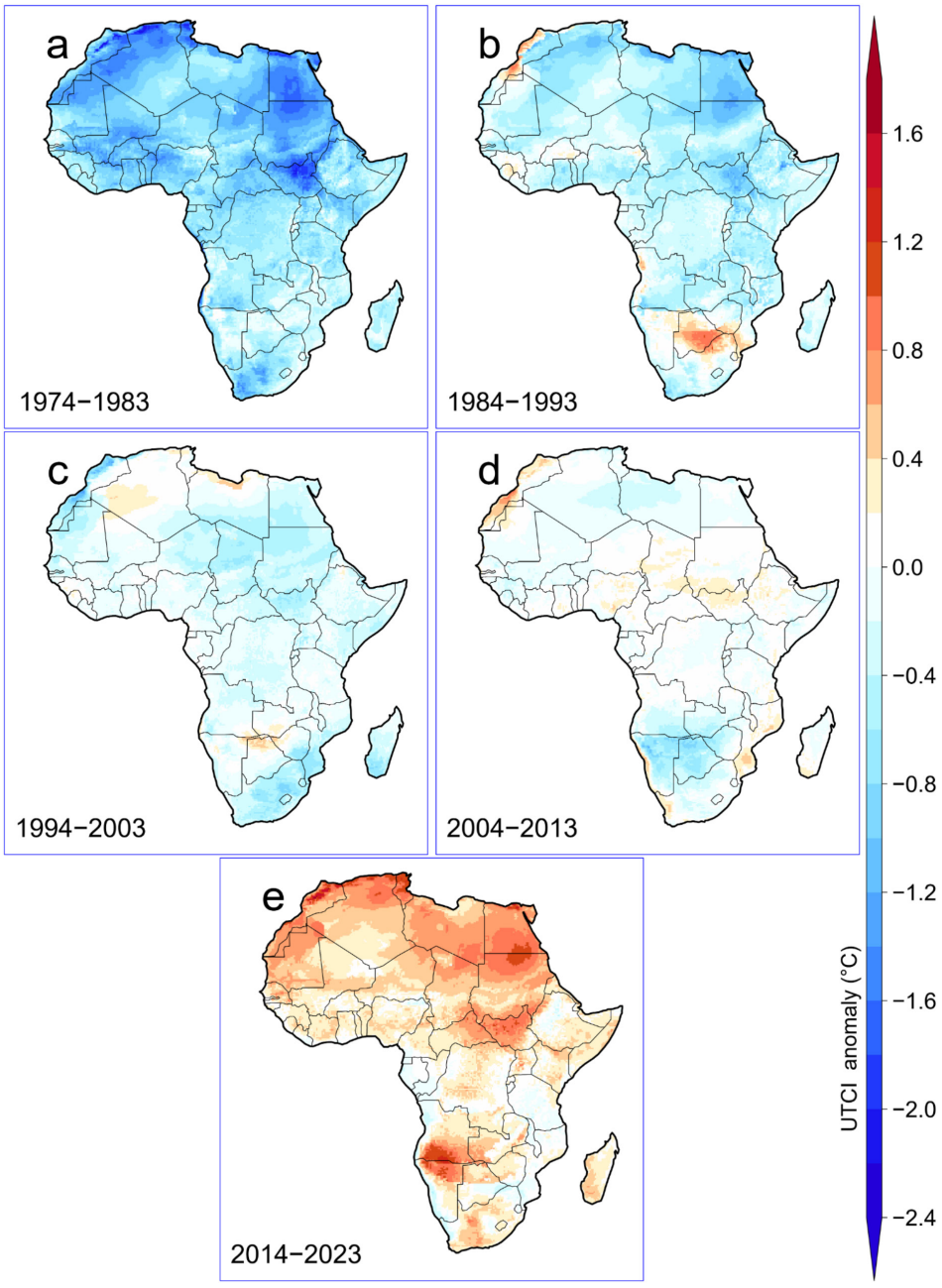

FIGURE 2 | Maximum UTCI has been increasing spatio-temporally between 1974 and 2023. Spatial patterns of summertime maximum UTCI anomalies across Africa at decade scale, relative to the 30-year summer average (1991–2020) in (a) 1973–1983, (b) 1984–1993, (c) 1994–2003, (d) 2004–2013 and (e) 2014–2023. [Colour figure can be viewed at wileyonlinelibrary.com]

plot). These years of intensified UTCI conditions during 1984–1993 suggest evidence of strong El Niño influence, which acts to shift the average summer thermal condition to 'very strong' heat stress, particularly, in South Africa, Botswana and Namibia (e.g., Roffe et al. 2023). This pattern is similar for 1994–2003, but relatively less intense. There is also a transition around this decade, with more normal and slightly warmer summer conditions across the continent.

Warming trends, reflected in positive summer UTCI values, intensified and expanded geographically during 2004–2013. However, Southern Africa exhibited a contrasting pattern, likely linked to the influence of strong La Niña phases during this period. In the subsequent decade (2014–2023), warming became more pronounced relative to the 30-year summer average, particularly across Northern Africa and regions like Namibia and Angola in the south. This acceleration aligns with studies attributing recent summertime heat extremes to human-induced global warming, which has intensified regional thermal stress. Previous studies (Lelieveld et al. 2016; Zittis et al. 2021) emphasise the role of anthropogenic drivers in exacerbating heat extremes; for instance, marginal global temperature increases significantly elevate thermal stress in Northern Africa, underscoring the region's vulnerability (Hamed et al. 2024). Additionally, land-use transitions, such as shifts between dominant land-cover classes, have been shown to either mitigate or amplify UTCI values in various regions (Adeyeri et al. 2023), highlighting the relationship between human activity and thermal stress/comfort.

Between the early and recent decades, UTCI anomaly trends appear more stable, though localised warming and cooling anomalies remain. These patterns are further supported by time series charts of UTCI anomalies for individual grid-specific summer seasons (Figure S5). The time series indicates an increase in UTCI anomalies, transitioning from negative to positive in the first decade, followed by a period of relative stability until after 2013, when positive UTCI anomalies continue to rise. This trend is consistent across all summer month groups, except for the OND summer area, which remains balanced in the early years.

3.3 | Trends in Consecutive Days of Heat Stress Per Year

The spatial pattern of consecutive heat stress days shown in Figure 3a reveals specific locations of prolonged heat stress conditions. Generally, without classifying the severity of the heat stress (i.e., 'All' heat stress), there appears to be a continent-wide homogeneity in the number of occurrences per duration category, although higher occurrences are observed in the Northern Hemisphere compared to the Southern Hemisphere. Limited occurrences are evident along the Great Lakes region of Africa, indicating the significant influence of water bodies in moderating temperatures in this area, although, with continued warming, increased heat stress in the region by the end of the century is very likely (Asefi-Najafabady et al. 2018).

Two distinct prolonged-intensity patterns emerged between the Northern and Southern Hemispheres when we classified heat stress by both duration and intensity. In the Southern Hemisphere, extended periods of 'strong' heat stress were more common. In contrast, the Northern Hemisphere experienced more frequent and prolonged episodes of 'very strong' and 'extreme' heat stress, with 'extreme' events occurring most prominently in the northernmost part of the Sahel region.

Using the spatial average for the entire African continent, we examined decadal variations in the number of occurrences across heat stress categories and durations (Figure 3b). We found that a non-classified analysis of heat stress conditions fails to reveal important patterns of variation across the region. For instance, there was no clear decadal variation in the average number of consecutive heat stress days for UTCI ≥ 32°C. This is evident from the relatively even distribution of consecutive heat stress days observed in the interannual variation (Figure S6).

However, when the data were disaggregated by heat stress categories and decades, a decline was observed in the number of 'strong' heat stress (32°C–38°C) events across all duration categories. Specifically, the number of occurrences declined from 16 to 11, 7 to 4 and 3 to 2 from the first decade (1974–1983) to the fifth decade (2014–2023) under 3–5, 6–8 and 9–12 days durations, respectively. In contrast, the number of occurrences of 'extreme' heat stress events (≥ 46°C) has doubled over the same period, increasing from 4 to 8 and from 2 to 4, particularly, under the 3–5 and 6–8 days duration categories.

3.4 | Quantifying Changes in the Spatial Extent of Persistent Heat Stress Days

We further examined the spatial trend to identify changes in the occurrence of heat stress over the 50-year period. By identifying the statistically significant grids, the uncorrected proportions (Figure S7) of change are consistent with those adjusted using the Benjamini–Hochberg FDR (Figure 4). For FDR-adjusted, 0.1%–4.1% of Africa experienced a significant increase in the days of consecutive 'strong' to 'extreme' heat stress (≥ 32°C) for different durations. Like the decadal variation, this, however, does not capture the variation in the changes for the different heat stress levels. Splitting the trend for the different ranges, the results showed a significant decrease in the occurrence of 'strong' heat stress across the durations. For 3–5, 6–8 and 9–13 days, 7%–18% of Africa experienced a significant decrease in the 'strong' heat stress, which was predominant across the Western region and parts of Central Africa (values reaching −0.2 event per year). During the same period, some parts of central to East Africa, however, experienced a significant increase in the occurrence of 'strong' heat stress. These regions experienced fewer occurrences of consecutive 'very strong' to 'extreme' heat stress days, suggesting a shift in heat stress patterns towards more frequent periods of consecutive heat stress.

For 'very strong' heat stress (38°C–46°C), we observed significant increases across western and central parts of Africa. In contrast, the Sahel region experienced a notable decline in this category, while parts of Northern Africa showed significant increases in the frequency and extent of 'very strong' heat stress events. Compared to the 'strong' heat stress condition, there was a decline in the areas where 'very strong' heat stress occurred over Africa. Specifically, it declined from 18% to 14.9%, 12.5% to 9% and 7% to 5.3% for the 3–5, 6–8 and 9–12 days duration category, respectively. 'Very strong' heat stress occurrence, however, increased over more areas revealed by the 14.3%, 9.9% and 5.4% increase from the strong heat stress duration of 3–5, 6–8 and 9–12 days, respectively. This is indicative of a shift in the heat stress occurrences over the continent of Africa, as 'very strong' heat stress conditions are lasting for more days than before. The occurrence of dangerous levels of heat stress, indicated by the 'extreme' heat stress category (≥ 46°C), has also become more pronounced in the Sahel region. About 14.9% of Africa has experienced a significant increase in the occurrence of consecutive extreme heat stress within 3–5 days duration. For longer periods, this has increased in about 7.6% and 1.1% of the continent for 6–8 and 9–12 days, respectively.

3.5 | Changes in HSH Over Continental Africa

This section analyses changes in hourly durations of grid-specific summer exposure to 'strong' or higher heat stress (UTCI ≥ 32°C) across Africa from 1974 to 2023, as shown in Figure 5a,b. Positive values reflect a significant rise in UTCI ≥ 32°C h, while negative values indicate a significant decline—both consistent with trends in Figure 5a, while Figure 5b,c shows the statistically significant grid cells

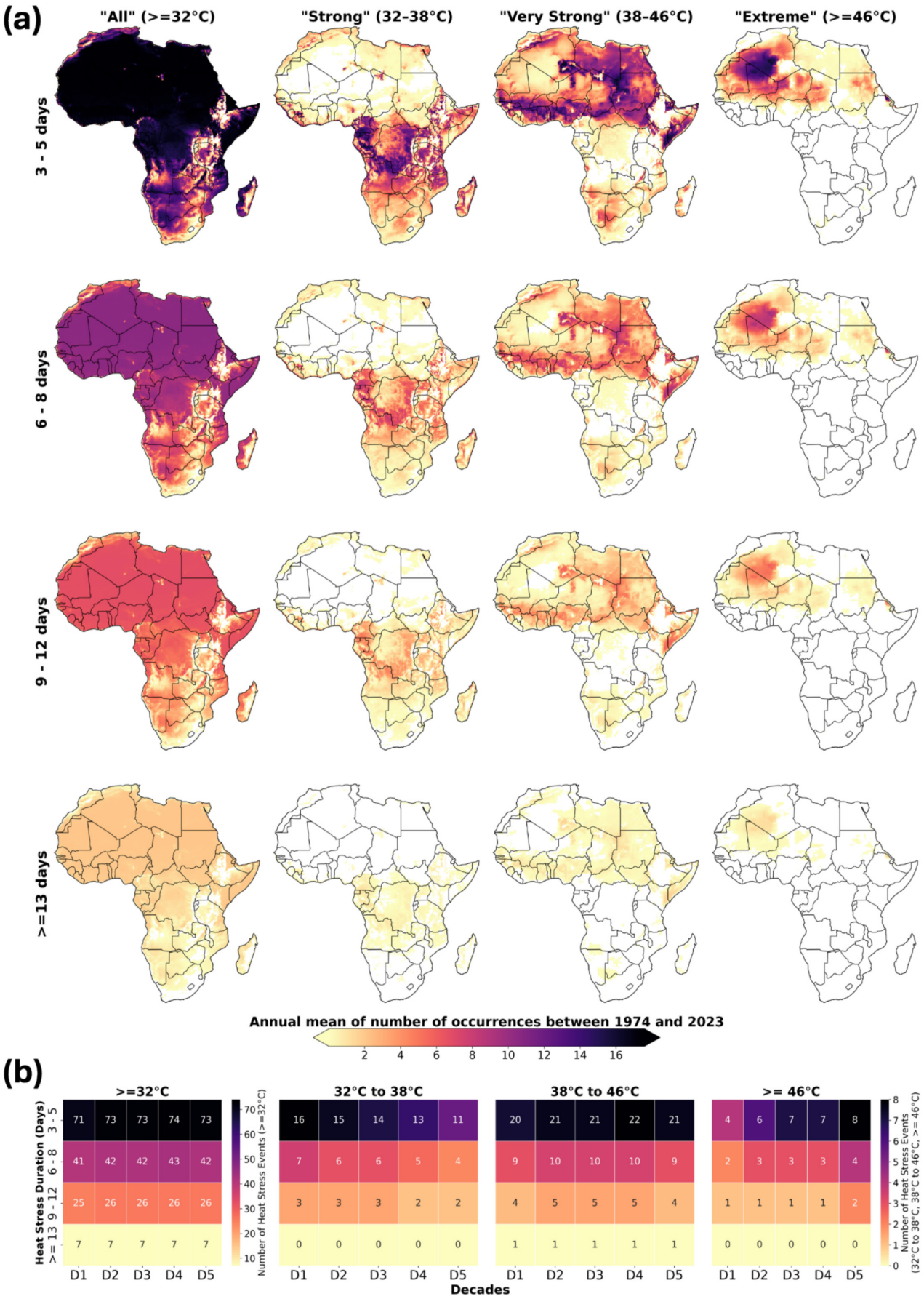

FIGURE 3 | Legend on next page.

FIGURE 3 | Duration and intensity of heat stress across the study period. (a) Climatological mean number of non-overlapping consecutive heat stress days for different UTCI categories. The ≥13 days category represents events lasting 13–30 days; (b) decadal count of consecutive heat stress events by intensity and duration from 1974 to 2023, grouped by decades: D1 (1974–1983), D2 (1984–1993), D3 (1994–2003), D4 (2004–2013) and D5 (2014–2023). Each panel corresponds to a UTCI heat stress category from left to right: 'All' (UTCI ≥ 32°C), 'Strong', 'Very Strong' and 'Extreme'. [Colour figure can be viewed at wileyonlinelibrary.com]

($p\_adj < 0.05$) identified using the Benjamini–Hochberg FDR method to account for multiple comparisons. Gridded overlays identify areas that have undergone statistically significant changes, as determined at the 95% confidence level. Generally, HSHs have increased across a large portion of the continent, with the percentage of hours where UTCI exceeds 32°C rising by more than 9% in many regions. The rise is most noticeable in northern Africa, especially in Niger, Mali, Mauritania, Chad and Sudan and in southern Africa, especially in Botswana, Namibia and South Africa (Ncongwane, Botai, Sivakumar, Botai, et al. 2021) and projections of intensifying heat stress over West and Central Africa (Dajuma et al. 2024) and Northern Africa (Hamed et al. 2024; Adeyeri, Ajadi, et al. 2025). However, a slight decline in HSHs is observed along the coastal regions of Namibia and Mozambique. Coastal regions under mild temperatures may experience less intense heat stress due to the cooling effects of sea breezes and other local climatic influences (Roffe et al. 2023). Long-term trends suggest a shift in heat exposure patterns, with implications for heat stress management and public health interventions (Tuholske et al. 2021).

Additionally, complementary bootstrap-based significance assessments (uncorrected and FDR-adjusted) highlight that the raw change field and the consistent spatial pattern across all significance frameworks provide compelling, high-confidence evidence of a pervasive, climate-driven rise in extreme heat exposure affecting major population centers and ecologically sensitive regions from 1974 to 2023.

3.6 | Changes in HSHs in Most Populated African Cities

Focusing on the city-specific changes, we examined the interannual heat stress for the hours per year when UTCI ≥ 32°C during the study period (Figure 5d) for the top 50 most populated cities (i.e., ≥1 million population). Generally, there was a significant increase in UTCI ≥ 32°C h per year in almost all cities, indicating an increase in the heat stress conditions since 1974. We grouped cities by their summer months and found that some of the highest changes were observed in cities with summer months from August to October, primarily located in Northern Africa, such as Alexandria (in Egypt), Algiers (in Algeria), Tunis (in Tunisia) and Tripoli (in Libya), which experienced significant increases of 7.6, 4.6, 4.2 and 3.4 h per year, respectively. Under other summer groupings, such as September to November, Dakar, Senegal increased significantly by 3.8 h per year. Kaduna, Nigeria experienced the highest increase from May to July at the rate of 2.6 h per year and Ibadan, Nigeria, from March to May at the rate of 2.8 h per year.

The number of occurrences of consecutive hours when UTCI ≥ 32°C per decade is presented in Figure 5e for the most populated city selected from each summer grouping. This represents the duration of heat stress and the variation for each decade. In most cities, the daily heat stress condition persisted for approximately 8–11 h during the summer. For example, in Cairo, Egypt, the frequency of heat stress occurrence for 10 consecutive hours was more than 200 times each decade; a similar observation was made at Kano, Nigeria and Suhag/Asiut, Egypt.

Comparing the occurrence of heat stress across the decades, an increase was observed in these cities, as 10 consecutive hours of heat stress became more frequent. In other cases, particularly 11 and 12 consecutive hours of heat stress, we observed an evolution of increased heat stress conditions. In most of the cities, there was a decline in the frequency of consecutive hours of heat stress over the decades. However, the frequency increased for 9–11 consecutive hours in Lagos, 10–12 consecutive hours in Kano, Cairo and Suhag/Asiut, 12–14 consecutive hours in Khartoum, Sudan and 7–9 consecutive hours in Lubumbashi, Congo. The occurrence of 9–12 consecutive hours of strong heat stress (UTCI ≥ 32°C) implies a large percentage of the day during the summer period is spent under at least 'strong' heat stress conditions. This indicates an increase in the very hot summers with associated discomfort for the inhabitants of these cities.

3.7 | Spatial and Temporal Changes in Population-Weighted Exposure

To assess temporal dynamics in human heat exposure, we analysed the daily number of people exposed to each heat stress category across Africa between 2000 and 2020 using gridded population data. This analysis captures both spatial shifts in exposure and the emergence of increasingly vulnerable populations.

Figure 6 illustrates the 20-year changes in population-weighted heat exposure, while Figure S8 shows 5-year progression patterns. Over the study period, there is a clear northward shift of populations exposed to higher heat stress categories. In some regions, particularly parts of the Sahel and Central Africa, the number of people experiencing 'strong' heat stress (UTCI = 32°C–38°C) per day declines. However, this does not indicate an overall reduction in exposure; rather, it reflects a transition of populations into higher-severity categories. Indeed, these same regions show substantial increases in daily exposure to 'very strong' heat stress (UTCI = 38°C–46°C) and 'extreme' heat stress (> 46°C), particularly in northern Africa and the Sahel.

Quantitatively, the percentage change in exposure between 2000 and 2020 (GPW population data) highlights this trend (Figure S9): for 'strong' heat stress, exposure increased by 51%, for 'very strong' by 86% and for 'extreme' by 158%. To assess the

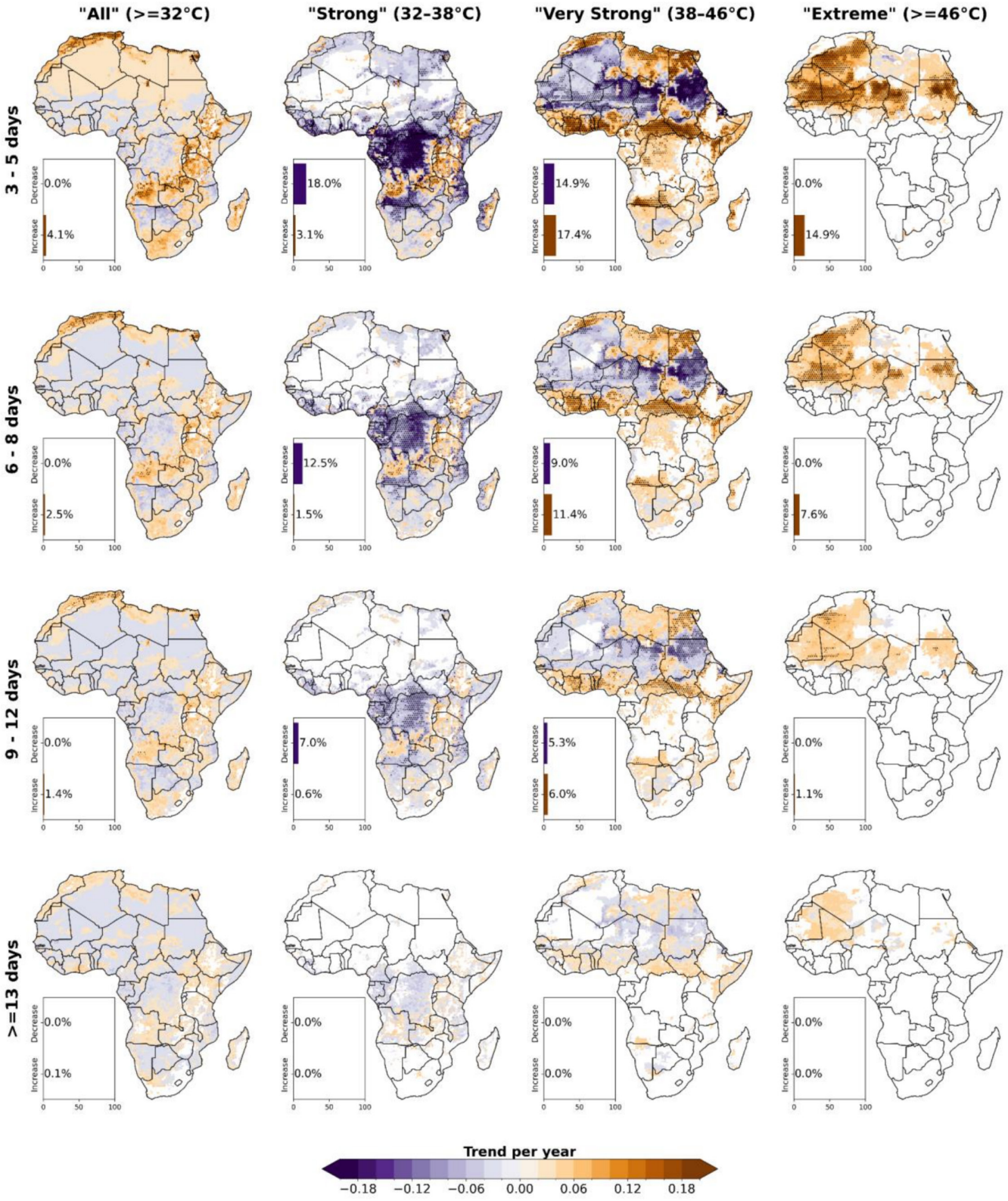

FIGURE 4 | Heat stress event trends for different UTCI categories and durations over the 50-year period from 1974 to 2023. The stripes represent the statistical significance (p-value < 0.05) identified using the Benjamini–Hochberg false discovery rate (FDR). Barplots represent the proportion of statistically significant grids relative to the total number of grids over Africa. [Colour figure can be viewed at wileyonlinelibrary.com]

robustness of these exposure estimates, we conducted a sensitivity analysis comparing results using GPWv4 and WorldPop population datasets. Overall, the spatial patterns and magnitude of exposure were highly consistent across datasets, with Pearson's correlation coefficients exceeding 0.89 for all years and categories. Detailed results of this sensitivity analysis are provided in Figures S9 and S10. These results demonstrate that ongoing warming trends are shifting daily heat stress extremes into

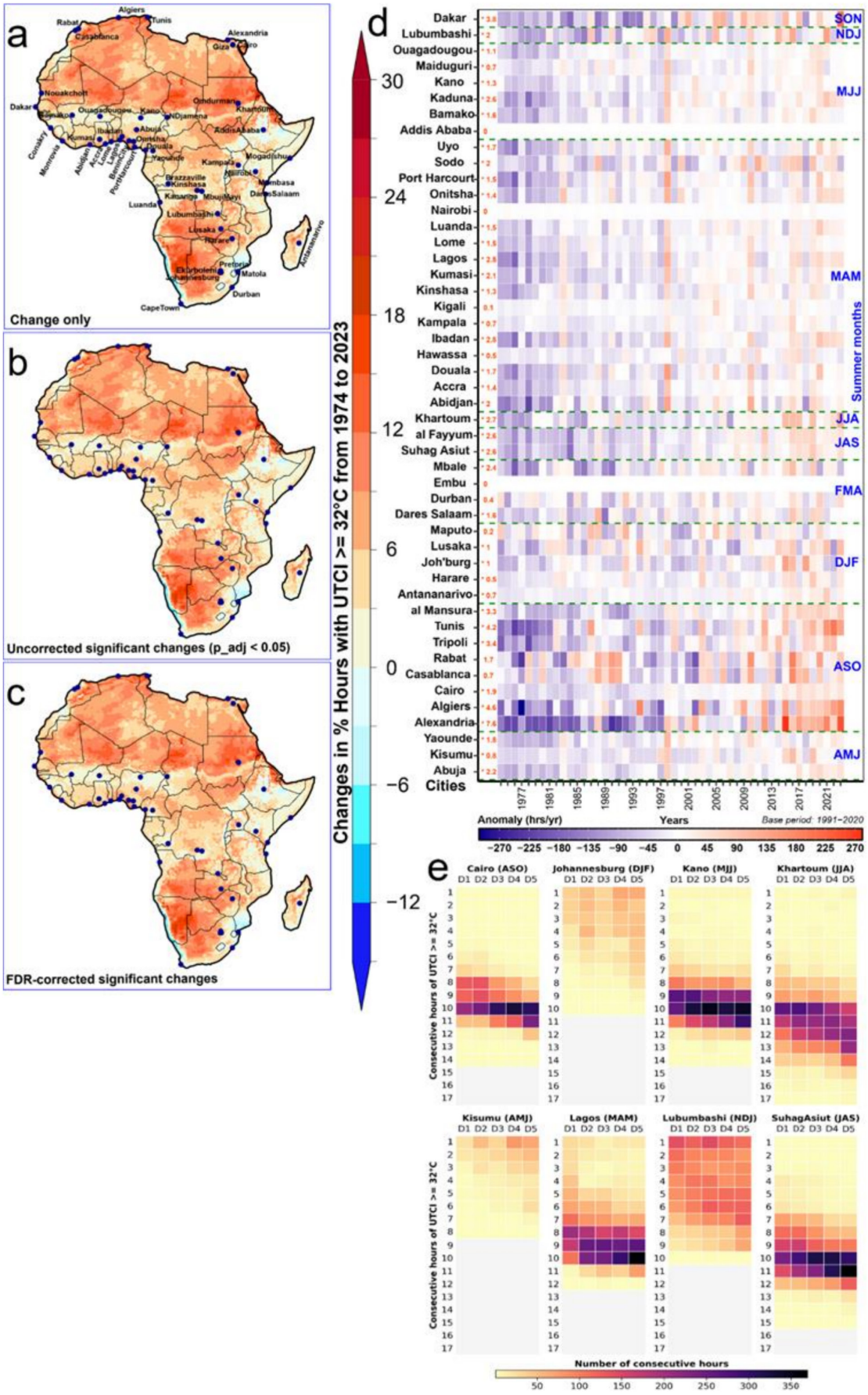

FIGURE 5 | Legend on next page.

FIGURE 5 | Hours of heat stressed hours has changed over time in Africa. (a–c) Change in the percentage of hours with UTCI ≥ 32°C across Africa from 1974 to 2023, with statistically significant grid cells (p_adj < 0.05) identified using the Benjamini–Hochberg false discovery rate (FDR) to account for multiple comparisons. The dots represent the cities. (d) Interannual variation in heat stress for the 50 most populated cities in Africa based on UTCI ≥ 32°C; (e) decadal count of consecutive hours with UTCI ≥ 32°C, grouped by decade: D1 (1974–1983), D2 (1984–1993), D3 (1994–2003), D4 (2004–2013) and D5 (2014–2023). Joh'burg in 5e means Johannesburg. [Colour figure can be viewed at wileyonlinelibrary.com]

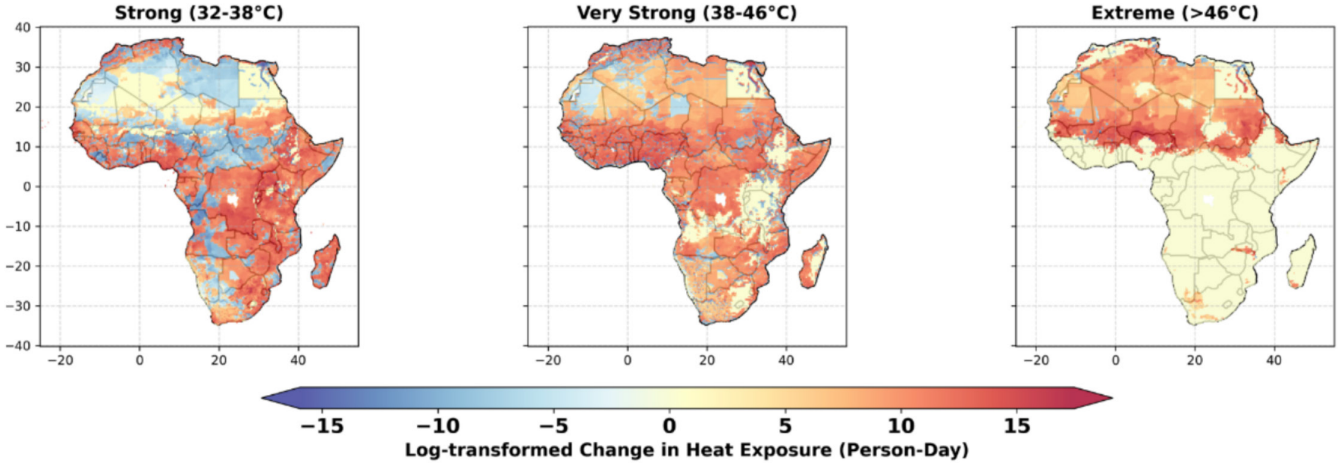

FIGURE 6 | Spatial patterns of changes in population heat exposure across Africa between 2000 and 2020, disaggregated by different UTCI-based heat stress categories. [Colour figure can be viewed at wileyonlinelibrary.com]

previously unrecorded ranges, exposing more people to higher-severity heat events (Matthews et al. 2017). The intensification and persistence of such exposures have serious public health implications, as prolonged extreme heat is strongly associated with increased morbidity, mortality and reduced labour capacity (Romanello et al. 2023).

4 | Discussion and Conclusions

4.1 | Summary and Key Findings

Heat is often mistakenly equated with high temperatures or heatwaves (McGregor and Vanos 2018). In human biometeorology, however, heat stress is a multifaceted phenomenon arising from the combined effects of air temperature, humidity, wind speed, solar and terrestrial radiation and metabolic activity (Błazejczyk et al. 2013; Di Napoli et al. 2021). The interaction of these factors with the human body determines the thermal load and resultant heat stress experienced, which can be objectively quantified using indices such as the UTCI. This study employs the UTCI derived from open-access ERA5-HEAT reanalysis data provided by the ECMWF Copernicus Climate Change Service (Di Napoli et al. 2021).

Historically, studies over Africa have explored heatwave patterns, extreme temperatures and population exposure at various scales. For instance, Moron et al. (2016) analysed trends in average temperatures (maximum and minimum) and hot extremes in tropical North Africa (1961–2014), highlighting a significant warming and an increase in heat episodes linked to climate change and large-scale oceanic influences. These results are consistent with Ringard et al. (2016), who found that the annual number of diurnal and nocturnal heatwaves increased over the Gulf of Guinea coastal regions during the second half of the 20th century, with an even stronger rise after the 1980s. Complementing these findings, Oueslati et al. (2017) demonstrated that heatwaves in the western Sahel are primarily driven by the water vapour greenhouse effect, while atmospheric circulation sustains these events through moisture advection from the adjacent Atlantic region. More recently, the focus has shifted towards impact-based analyses of heat stress. Research has examined spatio-temporal heat stress trends in specific regions (Adeyeri et al. 2023; Asefi-Najafabady et al. 2018; Fotso-Nguemo et al. 2022; Guigma et al. 2020; Hamed et al. 2024; Morakinyo et al. 2024; Ncongwane, Botai, Sivakumar, Botai, et al. 2021; Roffe et al. 2023), linking urbanisation, climate and land use change to rising thermal stress, noting more high-end heat stress days and increasing exposure—especially in West and Northeast Africa under high-emission scenarios.

This study advances the field by offering the first continent-wide, grid-specific assessment of summer heat stress climatology across Africa. We objectively examine the spatio-temporal patterns of heat stress at decadal, daily and hourly scales, covering multiple spatial scales—from continental to city levels. This comprehensive approach is novel, as it represents the first study to assess the long-term climatology of summer heat stress across the continent. Our results show regional differences in the timing and severity of peak heat stress: northern Africa experiences 'strong' to 'extreme' levels during peak hours, while southern regions typically face 'moderate' to 'strong' stress. Despite small absolute UTCI anomalies (< 2°C) over decades, substantial changes emerge at finer temporal scales. Notably, we observe a decline in the number of days with 'strong' heat stress, alongside increases in the frequency and duration of 'very strong' and 'extreme' events. At the hourly scale, most countries have experienced a rise in the number of hours exceeding 'strong'

heat stress. City-level analysis reveals seasonal variation in peak stress: MAM in West-to-East Africa, ASO in North Africa, DJF in Southern Africa and MJJ in the Sahel. Cities such as Cairo, Lagos, Kano and Suhag are experiencing longer and more frequent periods of severe heat stress.

Our results indicate that extreme heat stress is increasingly becoming the standard in numerous African regions. Since 1973, we have observed an increase in the intensity, frequency and spatial extent of heat stress—trends expected to persist through the century (Adeyeri et al. 2023; Dajuma et al. 2024; Fotso-Nguemo et al. 2022; Adeyeri, Ajadi, et al. 2025). Urban areas can be particularly vulnerable due to high population density and anthropogenic heat sources, especially during nighttime when UHI effects peak (Obe et al. 2024). Global exposure to temperatures exceeding human thermoregulatory limits, with tropical regions—particularly, in northern Africa and the Sahel—facing rapidly increasing exposure to 'extreme' heat stress conditions (>46°C) in current and future climate scenarios (Mora et al. 2017; Sylla et al. 2018; Tamoffo et al. 2025; Adeyeri, Ajadi, et al. 2025).

Atmospheric circulation changes and evolving heatwave dynamics further modulate regional exposure. Shifts in monsoon behaviour, wind systems and large-scale heat transport may be redistributing heat stress zones (Adeyeri et al. 2024), increasing risk even in historically less affected areas. Projected trends suggest a 12-fold expansion in areas affected by high-risk heat stress, with a 10%–30% increase in high-risk days and a 6%–20% rise in event intensity across West, Central and Northeast Africa (Fotso-Nguemo et al. 2022), a contraction of 'safe' thermal zones and an expansion of 'Caution' and 'Extreme Caution' zones across all seasons and emission pathways (Dajuma et al. 2024). The implications are severe: Prolonged exposure to extreme heat stress heightens the risk of heat-related illnesses, mortality and productivity loss, particularly among vulnerable groups such as the elderly, children and individuals with pre-existing health conditions. Although some argue for greater heat acclimatisation among African populations, recent analyses estimate over 13% (likely an underestimate due to data limitations) excess heat-related mortality due to rapid climate change and urbanisation (Zhao et al. 2021).

4.2 | Implication of Study and Recommendations for Mitigation and Adaptation

Heat stress exposure is highly unequal across Africa. Land-use and land-cover conditions strongly shape thermal risk; for example, non-forest land covers, particularly, primary and secondary types, are key drivers of elevated UTCI values (Adeyeri et al. 2023). This helps explain why rapidly urbanising regions such as the Sahel and parts of West Africa are increasingly experiencing sustained and recurrent exposure to high heat stress. Urbanisation further amplifies this burden through the UHI effect and associated land-surface modifications, meaning that heat vulnerability is often concentrated within cities.

Within urban areas, informal settlements, where more than half of sub-Saharan Africa's urban residents live, face disproportionate risks due to inadequate infrastructure, poor housing materials, limited public shade and restricted access to cooling and health services (Laue et al. 2022; Ncongwane, Botai, Sivakumar, Botai 2021). Informal-sector workers are especially exposed, with few resources or institutional protections to reduce heat impacts (Nunfam et al. 2020). Consequently, residents of low-income informal neighbourhoods often experience higher temperatures and increased susceptibility to heat-related outcomes such as heatstroke, hypertension, sleep disruption, skin disorders and psychosocial distress (Kunda et al. 2024; Scott et al. 2017). Yet evidence on these impacts remains fragmented, underscoring the need for integrated research to support policy and targeted interventions.

Effective heat-stress mitigation therefore requires a holistic strategy that addresses both climatic drivers and social determinants of vulnerability (Li et al. 2022; McGregor and Vanos 2018). We recommend multi-level Heat Action Plans spanning national, regional and city governance, supported by hybrid approaches that combine top-down policy with community-led implementation. Freetown, Sierra Leone, provides a pioneering example, having launched Africa's first heat action plan in 2025 to advance cooler, greener and more resilient urban environments. With over 70% of Africa's population projected to live in cities, similar strategies are urgently needed across the continent.

Key components should include climate-sensitive urban design that promotes ventilation through building orientation and street layout, reduces excessive compactness, deploys cool roofing and pavements, expands tree canopy and blue–green infrastructure and establishes accessible public cooling centres (Ng 2009; Wong et al. 2021). Importantly, strategies should be climate-zone specific. In hot-arid and Sahelian cities, priority actions include increasing surface reflectance in open areas using 'cool' materials, expanding shade through drought-tolerant urban forestry and applying water-efficient cooling measures (e.g., sub-surface irrigation, treated wastewater reuse or targeted misting at high-risk sites) where feasible (Schneider et al. 2023). In humid tropical cities, where high moisture limits evaporative cooling benefits, emphasis should be placed on shading, enhanced ventilation corridors, heat-resilient housing upgrades (reflective roofs, insulation, cross-ventilation) and the expansion of permeable and vegetated surfaces to reduce sensible heat storage. In temperate and highland cities, adaptation can focus on preventing rapid future risk escalation by protecting urban greenspaces, limiting heat-trapping infill and integrating heat considerations into urban growth plans.

Finally, early warning systems should move beyond national forecasts towards localised, community-centred heat alerts co-designed with local stakeholders to improve accessibility, risk communication and protective action (Brimicombe et al. 2021; Adegun et al. 2026). Together, these integrated measures are essential to safeguarding public health, sustaining productivity and strengthening urban resilience under continued warming.

4.3 | Limitation of Study Stemming From ERA5-HEAT

It is important to acknowledge spatial variability in the quality and confidence of the ERA5-HEAT dataset. Although

ERA5-HEAT benefits from a state-of-the-art data assimilation system and internally consistent model physics, its performance remains strongly dependent on the availability and density of assimilated observations. In observation-sparse regions such as parts of the developing world, oceanic areas, high-altitude environments and many parts of Africa where station networks are less dense than in North America or Europe, ERA5 (and by extension ERA5-HEAT) relies more heavily on model dynamics and parameterisations than on frequent observational corrections. As a result, uncertainties in key near-surface variables used to derive UTCI, particularly, wind speed and radiative fluxes, may introduce biases in UTCI estimates and affect the magnitude of derived trends (Krüger and Di Napoli 2022). Validation studies have similarly shown that reanalysis-based UTCI can exhibit larger local biases in absolute values where in situ observations are limited (Di Napoli et al. 2021; Morakinyo et al. 2024; Urban et al. 2021). Consistent with this, the ERA5-HEAT product evaluation reports a comparison of UTCI against 177 meteorological stations from the surface synoptic observations (SYNOP) network. It shows strongest performance in data-rich regions (Europe and North America). Across Africa, correlations are generally reported to exceed 0.6, albeit based on a comparatively sparse station network, with particularly limited coverage in Central and Eastern Africa (Di Napoli et al. 2021). Krüger and Di Napoli (2022) also report that, while mean bias may be lower outside summer, the spread in errors can be larger in fall and winter than in summer, indicating seasonally varying uncertainty.

In addition, the native spatial resolution of ERA5-HEAT (approximately 27 km) limits its ability to represent local-scale processes that shape thermal stress, particularly, MRT, in heterogeneous landscapes. Recent evaluation work suggests that ERA5-HEAT performs comparably to higher-resolution products over relatively flat terrain but is less accurate in complex terrain and in coastal or mountainous regions where microclimatic gradients are strong and sub-grid variability is high. Related analyses also highlight higher uncertainty and reduced precision in MRT estimates at elevated sites when compared with regional reanalyses such as CERRA (Skrynyk et al. 2025). Regional evaluations further indicate that ERA5 can reproduce near-surface temperature reasonably well in some West African coastal settings, such as Dakar and Abidjan and that interpolation can sometimes show slightly better agreement than alternative reanalyses such as MERRA (Ngoungue Langue et al. 2023). Taken together, these limitations suggest that ERA5-HEAT is best interpreted as providing spatially consistent, large-scale estimates of heat stress suitable for continental climatology and trend assessment, while local absolute UTCI values and trend magnitudes, especially in observation-sparse, complex-terrain or coastal environments, should be interpreted with appropriate caution.

Author Contributions

Tobi Eniolu Morakinyo: conceptualization, investigation, writing – originaldraft, methodology, validation, visualization, writing – review and editing, formal analysis, project administration, supervision. **Oluwafemi E. Adeyeri:** conceptualization, methodology, investigation, formal analysis, writing – original draft, writing – review and editing, validation, visualization, data curation. **Mojolaoluwa Toluwalase Daramola:** formal analysis, visualization, methodology, validation, conceptualization, investigation, writing – original draft, writing – review and editing. **Bobde Vishal:** investigation, writing – original draft, methodology, visualization, writing – review and editing, data curation, formal analysis. **Kazeem Abiodun Ishola:** conceptualization, investigation, writing – original draft, writing – review and editing, visualization, validation, methodology. **Oluwafemi Benjamin Obe:** conceptualization, investigation, writing – original draft, methodology, visualization, writing – review and editing, validation, formal analysis, data curation. **Emmanuel Olaoluwa Eresanya:** conceptualization, methodology, investigation, writing – original draft, writing – review and editing, formal analysis, visualization. **Akintomide Afolayan Akinsanola:** conceptualization, investigation, writing – original draft, writing – review and editing, validation, methodology, formal analysis, supervision. **Charles Onyutha:** writing – review and editing, validation. **Brian Odhiambo Ayugi:** writing – review and editing, validation. **Patricia Nying'uro:** writing – review and editing, validation.

Acknowledgements

We are grateful to the European Centre for Medium-Range Weather Forecasts (ECMWF) for free access to ERA5-HEAT reanalysis datasets. Oluwafemi E. Adeyeri is supported by Australian Research Council (Grant CE230100012). Emmanuel O. Eresanya is supported by the fellowship (Grant-Aid Agreement No. PDOC/23/01/04) with the support of the Marine Institute under the Marine Research Programme and funded by the Government of Ireland. In addition, the authors appreciate the efforts of the anonymous reviewers, whose constructive comments improved this paper. We also appreciate the editors for their time and support throughout the review process. Open access funding provided by Texas A&M University, College Station, is greatly appreciated.

Conflicts of Interest

The authors declare no conflicts of interest.

Data Availability Statement

The data that support the findings of this study are available in Corpernicus at https://doi.org/10.24381/cds.553b7518. These data were derived from the following resources available in the public domain: Corpernicus, https://cds.climate.copernicus.eu/datasets/derived-utci-historical?tab=download.

References

Adegun, O. B., T. E. Morakinyo, and P. Elias. 2026. "Designing and Evaluating a Community-Centred Heat Early Warning System (CHEWS) for Nigerian Slum Communities." *Urban Climate* 66: 102793.

Adeyeri, O. E., S. A. Ajadi, K. A. Ishola, and S. O. Mustapha. 2025. "The Societal Impact of Heatwave Intensification and Heat Stress on African Urban Populations." *Societal Impacts* 6: 100148. https://doi.org/10.1016/j.socimp.2025.100148.

Adeyeri, O. E., W. Zhou, P. Laux, et al. 2023. "Land Use and Land Cover Dynamics: Implications for Thermal Stress and Energy Demands." *Renewable and Sustainable Energy Reviews* 179: 113274. https://doi.org/10.1016/j.rser.2023.113274.

Adeyeri, O. E., W. Zhou, C. E. Ndehedehe, et al. 2025. "Asymmetric Heatwave Intensification Under Divergent Climate Change Mitigation Pathways Amplifies Urban–Rural Exposure Disparities." *Weather and Climate Extremes* 50: 100821. https://doi.org/10.1016/j.wace.2025.100821.

Adeyeri, O. E., W. Zhou, C. E. Ndehedehe, et al. 2025. "Global Heatwaves Dynamics Under Climate Change Scenarios: Multidimensional Drivers and Cascading Impacts." *Earth's Future* 13, no. 6: e2025EF006486.

Adeyeri, O. E., W. Zhou, C. E. Ndehedehe, and X. Wang. 2024. "Global Vegetation, Moisture, Thermal and Climate Interactions Intensify Compound Extreme Events." *Science of the Total Environment* 912: 169261. https://doi.org/10.1016/j.scitotenv.2023.169261.

Adigun, P., E. O. Abah, and O. D. Ajileye. 2024. "Intensifying Human-Driven Heatwaves Characteristics and Heat Related Mortality Over Africa." *Environmental Research: Climate* 3, no. 1: 015007. https://doi.org/10.1088/2752-5295/ad1f41.

Africapolis. 2025. "Africapolis." Accessed April 23, 2025. https://africapolis.org/en/data?menu=about.

Akinsanola, A. A., P. Singhai, T. N. Taguela, et al. 2025. "A Review of Urban Resilience to Weather and Climate Extremes." *City & Built Environment* 3, no. 1: 24.

Asefi-Najafabady, S., K. L. Vandecar, A. Seimon, P. Lawrence, and D. Lawrence. 2018. "Climate Change, Population, and Poverty: Vulnerability and Exposure to Heat Stress in Countries Bordering the Great Lakes of Africa." *Climatic Change* 148, no. 4: 561–573. https://doi.org/10.1007/s10584-018-2211-5.

Baldwin, J. W., T. Benmarhnia, K. L. Ebi, O. Jay, N. J. Lutsko, and J. K. Vanos. 2023. "Humidity's Role in Heat-Related Health Outcomes: A Heated Debate." *Environmental Health Perspectives* 131, no. 5: 55001. https://doi.org/10.1289/EHP11807.

Benjamin Obe, O., T. E. Morakinyo, and G. Mills. 2023. "Assessing Heat Risk in a Sub-Saharan African Humid City, Lagos, Nigeria, Using Numerical Modelling and Open-Source Geospatial Socio-Demographic Datasets." *City and Environment Interactions* 20: 100128. https://doi.org/10.1016/j.cacint.2023.100128.

Benjamini, Y., and Y. Hochberg. 1995. "Controlling the False Discovery Rate: A Practical and Powerful Approach to Multiple Testing.Journal of the Royal Statistical Society." *Series B (Methodological)* 57, no. 1: 289–300. https://doi.org/10.1111/j.2517-6161.1995.tb02031.x.

Błazejczyk, K., G. Jendritzky, P. Bröde, et al. 2013. "An Introduction to the Universal Thermal Climate Index (UTCI)." *Geographia Polonica* 86, no. 1: 5–10. https://doi.org/10.7163/GPol.2013.1.

Bobde, V., A. A. Akinsanola, and T. N. Taguela. 2025. "Future Intensification of Compound Heatwaves and Socioeconomic Exposure in Africa." *Earth's Future* 13, no. 12: 1–22.

Bobde, V., K. Ayegbusi, A. A. Akinsanola, O. E. Adeyeri, T. E. Morakinyo, and A. A. Adebiyi. 2025. "Anthropogenic Warming Is Accelerating Recent Heatwaves in Africa." *Communications Earth & Environment* 6, no. 1: 578.

Bonell, A., B. Sonko, J. Badjie, et al. 2022. "Environmental Heat Stress on Maternal Physiology and Fetal Blood Flow in Pregnant Subsistence Farmers in The Gambia, West Africa: An Observational Cohort Study." *Lancet Planetary Health* 6, no. 12: e968–e976. https://doi.org/10.1016/S2542-5196(22)00242-X.

Bonell, A., A. Vicedo-Cabrera, K. Murray, et al. 2023. "Assessing the Impact of Heat Stress on Growth Faltering in the First 1000 Days of Life in Rural Gambia." 1–16.

Brimicombe, C., C. Di Napoli, R. Cornforth, F. Pappenberger, C. Petty, and H. L. Cloke. 2021. "Borderless Heat Hazards With Bordered Impacts." *Earth's Future* 9, no. 9: 1–9. https://doi.org/10.1029/2021EF002064.

Bröde, P., D. Fiala, K. Błażejczyk, et al. 2012. "Deriving the Operational Procedure for the Universal Thermal Climate Index (UTCI)." *International Journal of Biometeorology* 56, no. 3: 481–494. https://doi.org/10.1007/s00484-011-0454-1.

Center For International Earth Science Information Network-CIESIN-Columbia University. 2018. "Gridded Population of the World, Version 4 (GPWv4): Population Density." Accessed April 23, 2025. https://doi.org/10.7927/H49C6VHW.

Dajuma, A., M. B. Sylla, M. Tall, et al. 2024. "Projected Intensification and Expansion of Heat Stress and Related Population Exposure Over Africa Under Future Climates." *Earth's Future* 12, no. 12: 1–23. https://doi.org/10.1029/2024EF004646.

Di Napoli, C., T. Allen, P. A. Méndez-Lázaro, and F. Pappenberger. 2023. "Heat Stress in the Caribbean: Climatology, Drivers, and Trends of Human Biometeorology Indices." *International Journal of Climatology* 43, no. 1: 405–425. https://doi.org/10.1002/joc.7774.

Di Napoli, C., C. Barnard, C. Prudhomme, H. L. Cloke, and F. Pappenberger. 2021. "ERA5-HEAT: A Global Gridded Historical Dataset of Human Thermal Comfort Indices From Climate Reanalysis." *Geoscience Data Journal* 8, no. 1: 2–10. https://doi.org/10.1002/gdj3.102.

Ebi, K. L., A. Capon, P. Berry, et al. 2021. "Hot Weather and Heat Extremes: Health Risks." *Lancet* 398, no. 10301: 698–708. Lancet. https://doi.org/10.1016/S0140-6736(21)01208-3.

Fiala, D., G. Havenith, P. Bröde, B. Kampmann, and G. Jendritzky. 2012. "UTCI-Fiala Multi-Node Model of Human Heat Transfer and Temperature Regulation." *International Journal of Biometeorology* 56, no. 3: 429–441. https://doi.org/10.1007/s00484-011-0424-7.

Fotso-Nguemo, T. C., D. A. Vondou, I. Diallo, et al. 2022. "Potential Impact of 1.5, 2 and 3 °C Global Warming Levels on Heat and Discomfort Indices Changes Over Central Africa." *Science of the Total Environment* 804: 150099. https://doi.org/10.1016/j.scitotenv.2021.150099.

Guigma, K. H., M. Todd, and Y. Wang. 2020. "Characteristics and Thermodynamics of Sahelian Heatwaves Analysed Using Various Thermal Indices." *Climate Dynamics* 55, no. 11–12: 3151–3175. https://doi.org/10.1007/s00382-020-05438-5.

Gyimah, R. R. 2023. "The Hot Zones Are Cities: Methodological Outcomes and Synthesis of Surface Urban Heat Island Effect in Africa." *Cogent Social Science* 9, no. 1: 1–11. https://doi.org/10.1080/23311886.2023.2165651.

Hamed, M. M., A. A. J. Al-Hasani, M. S. Nashwan, Z. Sa'adi, and S. Shahid. 2024. "Assessing the Growing Threat of Heat Stress in the North Africa and Arabian Peninsula Region Connected to Climate Change." *Journal of Cleaner Production* 447: 141639. https://doi.org/10.1016/j.jclepro.2024.141639.

Hersbach, H., B. Bell, P. Berrisford, et al. 2020. "The ERA5 Global Reanalysis." *Quarterly Journal of the Royal Meteorological Society* 146, no. 730: 1999–2049. https://doi.org/10.1002/qj.3803.

Igun, E., X. Xu, Y. Hu, and G. Jia. 2022. "Strong Heatwaves With Widespread Urban-Related Hotspots Over Africa in 2019." *Atmospheric and Oceanic Science Letters* 15, no. 5: 100195. https://doi.org/10.1016/j.aosl.2022.100195.

Kendall, M. G. 1948. *Rank Correlation Methods*. Charles Griffin.

Krüger, E. L., and C. Di Napoli. 2022. "Feasibility of Climate Reanalysis Data as a Proxy for Onsite Weather Measurements in Outdoor Thermal Comfort Surveys." *Theoretical and Applied Climatology* 149, no. 3–4: 1645–1658. https://doi.org/10.1007/s00704-022-04129-x.

Kunda, J. J., S. N. Gosling, and G. M. Foody. 2024. "The Effects of Extreme Heat on Human Health in Tropical Africa." *International Journal of Biometeorology* 68, no. 6: 1015–1033. https://doi.org/10.1007/s00484-024-02650-4.

Laue, F., O. B. Adegun, and A. Ley. 2022. "Heat Stress Adaptation Within Informal, Low-Income Urban Settlements in Africa." *Sustainability* 14, no. 13: 1–14. https://doi.org/10.3390/su14138182.

Lelieveld, J., Y. Proestos, P. Hadjinicolaou, M. Tanarhte, E. Tyrlis, and G. Zittis. 2016. "Strongly Increasing Heat Extremes in the Middle East and North Africa (MENA) in the 21st Century." *Climatic Change* 137, no. 1–2: 245–260. https://doi.org/10.1007/s10584-016-1665-6.

Li, X., L. C. Stringer, and M. Dallimer. 2022. "The Impacts of Urbanisation and Climate Change on the Urban Thermal Environment in Africa." *Climate* 10, no. 11: 1–21. https://doi.org/10.3390/cli10110164.

Mann, H. B. 1945. "Nonparametric Tests Against Trend." *Econometrica: Journal of the Econometric Society* 13: 245–259.

Manyuchi, A. E., C. Vogel, C. Y. Wright, and B. Erasmus. 2022. "The Self-Reported Human Health Effects Associated With Heat Exposure in Agincourt Sub-District of South Africa." *Humanities and Social Sciences Communications* 9, no. 1: 1–12. https://doi.org/10.1057/s41599-022-01063-1.

Matthews, T. K. R., R. L. Wilby, and C. Murphy. 2017. "Communicating the Deadly Consequences of Global Warming for Human Heat Stress." *Proceedings of the National Academy of Sciences of the United States of America* 114, no. 15: 3861–3866. https://doi.org/10.1073/pnas.1617526114.

McGregor, G. R., and J. K. Vanos. 2018. "Heat: A Primer for Public Health Researchers." *Public Health* 161: 138–146. https://doi.org/10.1016/j.puhe.2017.11.005.

Meque, A., I. Pinto, G. Maúre, and A. Beleza. 2022. "Understanding the Variability of Heatwave Characteristics in Southern Africa." *Weather and Climate Extremes* 38: 100498. https://doi.org/10.1016/j.wace.2022.100498.

Mitchell, B. C., J. Chakraborty, and P. Basu. 2021. "Social Inequities in Urban Heat and Greenspace: Analyzing Climate Justice in Delhi, India." *International Journal of Environmental Research and Public Health* 18, no. 9: 4800. https://doi.org/10.3390/ijerph18094800.

Mora, C., B. Dousset, I. R. Caldwell, et al. 2017. "Global Risk of Deadly Heat." *Nature Climate Change* 7, no. 7: 501–506. https://doi.org/10.1038/nclimate3322.

Morakinyo, T. E., K. A. Ishola, E. O. Eresanya, M. T. Daramola, and I. A. Balogun. 2024. "Spatio-Temporal Characteristics of Heat Stress Over Nigeria Using Evaluated ERA5-HEAT Reanalysis Data." *Weather and Climate Extremes* 45: 100704. https://doi.org/10.1016/j.wace.2024.100704.

Morakinyo, T. E., O. B. Obe, G. Mills, et al. 2026. "The Impact of Hazard Indicator Selection on Urban Heat Risk Assessment: Evidence From Two Sub-Saharan African Cities." *City and Environment Interactions* 30: 1–16. https://doi.org/10.1016/j.cacint.2026.100338.

Morakinyo, T. E., S. B. Ogungbenro, A. T. Abolude, and A. A. Akinsanola. 2019. "Quantifying the Effect of Rain Events on Outdoor Thermal Comfort in a High-Density City, Hong Kong." *International Journal of Biometeorology* 63, no. 1: 19–27. https://doi.org/10.1007/s00484-018-1634-z.

Moron, V., B. Oueslati, B. Pohl, S. Rome, and S. Janicot. 2016. "Trends of Mean Temperatures and Warm Extremes in Northern Tropical Africa (1961–2014) From Observed and PPCA-Reconstructed Time Series." *Journal of Geophysical Research: Atmospheres* 121, no. 10: 5298–5319.

Muheki, D., A. A. J. Deijns, E. Bevacqua, G. Messori, J. Zscheischler, and W. Thiery. 2024. "The Perfect Storm? Co-Occurring Climate Extremes in East Africa." *Earth System Dynamics* 15: 429–466. https://doi.org/10.5194/esd-15-429-2024.

Ncongwane, K. P., J. O. Botai, V. Sivakumar, and C. M. Botai. 2021. "A Literature Review of the Impacts of Heat Stress on Human Health Across Africa." *Sustainability* 13, no. 9: 5312. https://doi.org/10.3390/su13095312.

Ncongwane, K. P., J. O. Botai, V. Sivakumar, C. M. Botai, and A. M. Adeola. 2021. "Characteristics and Long-Term Trends of Heat Stress for South Africa." *Sustainability* 13, no. 23: 1–20. https://doi.org/10.3390/su132313249.

Ng, E. 2009. "Policies and Technical Guidelines for Urban Planning of High-Density Cities - Air Ventilation Assessment (AVA) of Hong Kong." *Building and Environment* 44, no. 7: 1478–1488. https://doi.org/10.1016/j.buildenv.2008.06.013.

Ngoungue Langue, C. G., C. Lavaysse, M. Vrac, and C. Flamant. 2023. "Heat Wave Monitoring Over West African Cities: Uncertainties, Characterization and Recent Trends." *Natural Hazards and Earth System Sciences* 23, no. 4: 1313–1333.

Nunfam, V. F., K. Adusei-Asante, K. Frimpong, E. J. Van Etten, and J. Oosthuizen. 2020. "Barriers to Occupational Heat Stress Risk Adaptation of Mining Workers in Ghana." *International Journal of Biometeorology* 64, no. 7: 1085–1101. https://doi.org/10.1007/s00484-020-01882-4.

Obe, O. B., T. E. Morakinyo, and G. Mills. 2024. "An Assessment of WRF-Urban Schemes in Simulating Local Meteorology for Heat Stress Analysis in a Tropical Sub-Saharan African city, Lagos, Nigeria." *International journal of biometeorology* 68, no. 5: 811–828.

Olaoluwa, E. E., O. S. Durowoju, I. R. Orimoloye, M. T. Daramola, A. A. Ayobami, and O. Olorunsaye. 2022. "Chapter 1—Understanding Weather and Climate Extremes." In *Climate Impacts on Extreme Weather*, edited by V. Ongoma and H. Tabari, 1–17. Elsevier. https://doi.org/10.1016/B978-0-323-88456-3.00008-3.

Oueslati, B., B. Pohl, V. Moron, S. Rome, and S. Janicot. 2017. "Characterization of Heat Waves in the Sahel and Associated Physical Mechanisms." *Journal of Climate* 30, no. 9: 3095–3115.

Parkes, B., J. R. Buzan, and M. Huber. 2022. "Heat Stress in Africa Under High Intensity Climate Change." *International Journal of Biometeorology* 66, no. 8: 1531–1545. https://doi.org/10.1007/s00484-022-02295-1.

Parkes, B., J. Cronin, O. Dessens, and B. Sultan. 2019. "Climate Change in Africa: Costs of Mitigating Heat Stress." *Climatic Change* 154, no. 3–4: 461–476. https://doi.org/10.1007/s10584-019-02405-w.

Ringard, J., B. Dieppois, S. Rome, et al. 2016. "The Intensification of Thermal Extremes in West Africa." *Global and Planetary Change* 139: 66–77.

Roffe, S. J., A. J. van der Walt, and J. M. Fitchett. 2023. "Spatiotemporal Characteristics of Human Thermal Comfort Across Southern Africa: An Analysis of the Universal Thermal Climate Index for 1971–2021." *International Journal of Climatology* 43, no. 6: 2930–2952. https://doi.org/10.1002/joc.8009.

Romanello, M., C. di Napoli, C. Green, et al. 2023. "The 2023 Report of the Lancet Countdown on Health and Climate Change: The Imperative for a Health-Centred Response in a World Facing Irreversible Harms." *Lancet* 402, no. 10419: 2346–2394. https://doi.org/10.1016/S0140-6736(23)01859-7.

Schneider, F. A., J. C. Ortiz, J. K. Vanos, D. J. Sailor, and A. Middel. 2023. "Evidence-Based Guidance on Reflective Pavement for Urban Heat Mitigation in Arizona." *Nature Communications* 14, no. 1: 1–12. https://doi.org/10.1038/s41467-023-36972-5.

Scott, A. A., H. Misiani, J. Okoth, et al. 2017. "Temperature and Heat in Informal Settlements in Nairobi." *PLoS One* 12, no. 11: e0187300.

Sen, P. K. 1968. "Estimates of the Regression Coefficient Based on Kendall's Tau." *Journal of the American Statistical Association* 63, no. 324: 1379–1389.

Skrynyk, O., P. Nejedlík, and K. Błażejczyk. 2025. "Intermodel and Method Comparison of Mean Radiant Temperature From Numerical Weather Prediction Models: Evaluation of Enhanced Spatial Resolution in Europe." *Contributions to Geophysics & Geodesy* 55, no. 2: 181–200.

Sylla, M. B., A. Faye, F. Giorgi, A. Diedhiou, and H. Kunstmann. 2018. "Projected Heat Stress Under 1.5 °C and 2 °C Global Warming Scenarios Creates Unprecedented Discomfort for Humans in West Africa." *Earth's Future* 6, no. 7: 1029–1044. https://doi.org/10.1029/2018EF000873.

Tamoffo, A. T., T. Weber, and F. Saleem. 2025. "Population Exposed to Compound Extreme Hot & Humid and Wet & Windy Events in Africa."

Environmental Research Letters 20, no. 1: 014038. https://doi.org/10.1088/1748-9326/ad9d5f.

Theil, H. 1992. "A Rank-Invariant Method of Linear and Polynomial Regression Analysis." In *Henri Theil's Contributions to Economics and Econometrics: Econometric Theory and Methodology*, 345–381. Springer.

Tuholske, C., K. Caylor, C. Funk, et al. 2021. "Global Urban Population Exposure to Extreme Heat." *Proceedings of the National Academy of Sciences of the United States of America* 118, no. 41: 1–9. https://doi.org/10.1073/pnas.2024792118.

Ullah, S., A. Aldossary, W. Ullah, and S. G. Al-Ghamdi. 2024. "Augmented Human Thermal Discomfort in Urban Centers of the Arabian Peninsula." *Scientific Reports* 14, no. 1: 1–17. https://doi.org/10.1038/s41598-024-54766-7.

Urban, A., C. Di Napoli, H. L. Cloke, et al. 2021. "Evaluation of the ERA5 Reanalysis-Based Universal Thermal Climate Index on Mortality Data in Europe." *Environmental Research* 198: 111227. https://doi.org/10.1016/j.envres.2021.111227.

Vecellio, D. J., Q. Kong, W. L. Kenney, and M. Huber. 2023. "Greatly Enhanced Risk to Humans as a Consequence of Empirically Determined Lower Moist Heat Stress Tolerance." *Proceedings of the National Academy of Sciences of the United States of America* 120, no. 42: 1–9. https://doi.org/10.1073/pnas.2305427120.

Wong, N. H., C. L. Tan, D. D. Kolokotsa, and H. Takebayashi. 2021. "Greenery as a Mitigation and Adaptation Strategy to Urban Heat." *Nature Reviews Earth and Environment* 2, no. 3: 166–181. https://doi.org/10.1038/s43017-020-00129-5.

Zhao, Q., Y. Guo, T. Ye, et al. 2021. "Global, Regional, and National Burden of Mortality Associated With Non-Optimal Ambient Temperatures From 2000 to 2019: A Three-Stage Modelling Study." *Lancet Planetary Health* 5, no. 7: e415–e425. https://doi.org/10.1016/S2542-5196(21)00081-4.

Zittis, G., P. Hadjinicolaou, M. Almazroui, et al. 2021. "Business-As-Usual Will Lead to Super and Ultra-Extreme Heatwaves in the Middle East and North Africa." *npj Climate and Atmospheric Science* 4, no. 1: 20. https://doi.org/10.1038/s41612-021-00178-7.

Supporting Information

Additional supporting information can be found online in the Supporting Information section. **Figure S1:** Spatial variation of minimum heat stress conditions across decades and period of study (1974–2023). **Figure S2:** Spatial variation of mean heat stress conditions across decades and period of study (1974–2023). **Figure S3:** Spatial variation of maximum heat stress conditions across decades and period of study (1974–2023). **Figure S4:** Spatial patterns of summertime ERA5-HEAT maximum UTCI anomalies (1974–2023) across Africa, relative to the 30-year summer average (1974–2023). **Figure S5:** Temporal patterns of ERA5-HEAT maximum UTCI anomalies (1974–2023) for each grid-specific summer season across Africa, relative to the 30-year summer average (1991–2020). **Figure S6:** Interannual plots of UTCI heat stress events under different categories and durations from 1974 to 2023 **Figure S7:** Heat stress event trends for different UTCI categories and durations over the 50-year period from 1974 to 2023. **Figure S8:** Spatial pattern of population heat exposure for different categories of heat stress. **Figure S9:** (a) Population-weighted exposure based on GPWv4 and WorldPop population datasets for 2000, 2010 and 2020 for each heat stress category. (b) Percent difference between the population-weighted exposure based on GPWv4 and WorldPop. **Figure S10:** summarises the spatial correspondence between GPW- and WorldPop-based exposures. **Figure S10:** Spatial correlation between GPW- and WorldPop-based exposures.